

# PAMELA Satellite Data as a Signal of Non-Thermal Wino LSP Dark Matter

Gordon Kane,<sup>\*</sup> Ran Lu,<sup>†</sup> and Scott Watson<sup>‡</sup>

*Michigan Center for Theoretical Physics, University of Michigan, Ann Arbor, Michigan 48109, USA*

Satellite and astrophysical data is accumulating that suggests and constrains interpretations of the dark matter of the universe. We argue there is a very well motivated theoretical framework (which existed before data) consistent with the interpretation that dark matter annihilation is being observed by the PAMELA satellite detector. The dark matter is (mainly) the neutral W boson superpartner, the wino. Using the program GALPROP extensively we study the annihilation products and the backgrounds together. A wino mass approximately in the 180 – 200 GeV range gives a good description of the PAMELA data, with antimatter and gammas from annihilating winos dominating the data below this energy range but not contributing above it. We explain why PAMELA data does not imply no antiproton signal was observed by PAMELA or earlier experiments, and explain why the antiproton analysis was misunderstood by earlier papers. Wino annihilation does not describe the Fermi  $e^+ + e^-$  data (except partially below  $\sim 100$  GeV). At higher energies we expect astrophysical mechanisms to contribute, and we simply parameterize them without a particular physical interpretation, and check that the combination can describe all the data. We emphasize several predictions for satellite data to test the wino interpretation, particularly the flattening or turndown of the positron and antiproton spectra above 100 GeV. It should be emphasised that most other interpretations require a large rise in the positron and antiproton rates above 100 GeV. We focus on studying this well-motivated and long predicted wino interpretation, rather than comparisons with other interpretations. We emphasize that interpretations also depend very strongly on assumptions about the cosmological history of the universe, on assumptions about the broader underlying theory context, and on propagation of antiprotons and positrons in the galaxy. The winos PAMELA is observing arose from moduli decay or other non-thermal sources rather than a universe that cooled in thermal equilibrium after the big bang. Then it is appropriate to normalize the wino density to the local relic density, and no “boost factors” are needed to obtain the reported PAMELA rates.

## I. INTRODUCTION

How does one learn what physics interpretation to give to tentative signals of antimatter and gammas in the galaxy? Could it be due to annihilating dark matter? Answering this is not straightforward – it strongly depends on assumptions that are not always made explicit, and the answer is also very sensitive to assumptions about propagation in the galaxy, and to parameters used to describe the propagation. Perhaps surprisingly, assumptions about cosmological history are crucial. It also depends on whether more than one mechanism is providing the signals.

As the recent PAMELA and then Fermi satellite data appeared, essentially everyone who studied it assumed that the universe cooled in thermal equilibrium after the big bang (dark matter particles  $\chi$  annihilated into Standard Model particles, which could annihilate back into dark matter particles if they had enough energy, until the cooling led to freeze-out of the dark matter at some relic density). Then the relic density is  $\rho \approx H/\langle\sigma v\rangle$ , where the Hubble parameter  $H$  is evaluated at the freeze-out temperature (about  $M_\chi/25$ ). This remarkable formula, with the relic density depending only on the cosmological Hubble parameter and on the weak scale annihilation rate, has been called the “wimp miracle”. Getting the correct relic density implied that  $\langle\sigma v\rangle \approx 3 \times 10^{-26} \text{ cm}^3\text{s}^{-1}$ , so any candidate with a larger annihilation cross section was excluded. In recent years, however, it has become increasingly clear that comprehensive underlying theories which explain more than one thing at a time generically have additional sources of dark matter, such as decaying particles, and therefore that assuming thermal equilibrium as the universe cools is oversimplified and misleading. This was noticed in [1, 2, 3], emphasized a decade ago by Moroi and Randall[4], and more recently documented in detail in a model based on a string theory construction with M theory compactified on a manifold with  $G_2$  holonomy[5]. See also [6].

Further, the standard assumption of most studies was that a single candidate had to describe the data for electrons, positrons, antiprotons, and gammas at all energies. It’s not clear why one would assume that, since in the presence

---

<sup>\*</sup>Electronic address: gkane@umich.edu

<sup>†</sup>Electronic address: luran@umich.edu

<sup>‡</sup>Electronic address: watsongs@umich.edu

of dark matter there will in general be contributions from the annihilating dark matter, and also from several astrophysical sources such as interstellar medium accelerated by supernova remnant shock waves, pulsars, and perhaps more. In some theories the dark matter is metastable, its decay induced by much higher dimension operators, and contributes *both* via annihilation and via decay (work in progress)

Dark matter composed of the lightest superpartner has been a very well motivated candidate for all or part of the dark matter of the universe for nearly three decades. The dark matter annihilation cross section is of order  $\sigma \sim \alpha_2/M_{\chi}^2$ , where  $\alpha_2$  is the weak coupling. In the past decade the particular possibility where the dark matter is mainly the partner of the W boson, the wino, has been very well motivated in any theory where supersymmetry is broken by the anomaly mediation mechanism [7], or more generally where the anomaly mediation contribution to gaugino masses is comparable with other sources of gaugino masses (as in the  $G_2$  construction), and in other approaches such as U(1) mediation [8]. In a universe where the relic density emerged in thermal equilibrium the wino mass had to be of order 2 TeV to get the right relic density. But in the non-thermal universes where the dark matter mainly arose from decay of additional particles, such as the moduli generically present in any string theory, the correct temperature at which to evaluate the Hubble parameter was the moduli decay or reheating temperature. This is quite different from the freeze-out temperature [4, 5, 6]. Then the correct relic density emerged for wino masses of order 200 GeV, for which  $\langle\sigma v\rangle \simeq 3 \times 10^{-24} \text{ cm}^3\text{s}^{-1}$ . Although the winos arise continuously as the moduli decay, rather than the superpartners being mainly present at the big bang, a "non-thermal wimp miracle" still occurs when the scaling of the Hubble parameter and cross section with temperature and mass are taken into account [4, 5, 6].

Remarkably, this 200 GeV mass scale is just the one that is right for the PAMELA data. In a universe where the relic density arises non-thermally, as generically in string theories, a wino LSP with relic density normalized to the observed local relic density ( $0.3 \text{ GeV}/\text{cm}^3$ ) gives about the amount of positrons and antiprotons (and their distributions) reported in the PAMELA experiment! No "boost factor" is needed.

Positrons and antiprotons have long resident times in the galaxy, millions of years. In order to compute the number of events as functions of energy that PAMELA and Fermi should observe one needs to include all the effects of propagation in the galaxy. There are two main programs to facilitate that, GALPROP[9] and DarkSUSY[10, 11], each valuable for somewhat different calculations. Here we use GALPROP since we need to have one program that treats the signal and background particles in a self-consistent manner as they are affected by the galactic magnetic fields, lose energy by synchrotron radiation, inverse Compton scattering, collisions, escape the galactic disk, etc. As we will explain, this is crucial for understanding the antiprotons, where we argue that use of parameterized backgrounds has led people incorrectly to assume that PAMELA was not seeing an annihilation signal in antiprotons.

We find that in the PAMELA region the results can depend significantly on a number of astrophysical parameters (see Table I), and that there are many degeneracies and flat directions among the parameters. The GALPROP running time is long, of order several hours, so we have not yet been able to do full parameter scanning. Improved computing, and additional constraints from satellite data that should be reported in the next few months, should improve this situation significantly. It should be emphasized that the positrons and antiprotons "injected" into the galaxy by pure wino annihilation have no parameters apart from the mass scale, which can only vary at the 5-10% level. All the issues about describing the data arise from the propagation.

If annihilation of LSP dark matter is the origin of the excess positrons, it obviously must give excess antiprotons since all MSSM states will include quarks and antiquarks in their annihilation products, and the antiquarks fragment into antiprotons. In particular, for the wino LSP the annihilation of winos is to  $W^+ + W^-$ , and the W-bosons have known branching ratios to leptonic and quark final states, and the probability they will give antiprotons was measured at LEP. The relevant processes are incorporated into PYTHIA and we use them. There is no freedom. This has led to many statements in literature that the apparent absence of an antiproton excess excludes MSSM LSP models, and in particular excludes wino annihilation as the explanation of the positron excess, and forces one to approaches that only give leptons. It turns out that these conclusions are wrong, for three interesting reasons. First, the antiproton spectrum from quark fragmentation is significant down to quite soft antiprotons, and it gives a significant number of antiprotons in the 1 – 10 GeV region and even below. The positron spectrum from W's has many energetic positrons at higher energies, and is peaked at higher energies than the antiproton spectrum. Second, the antiprotons do not lose much energy as they propagate compared to the positrons, so the GeV antiprotons are detected by PAMELA, while the positrons lose energy readily and the soft ones do not make it to the detector. This can be seen from the figures below, where the signal from antiprotons is above the background down to the lowest energies, while the positron signal is at the background level below about 5 GeV, and essentially gone below 10 GeV. Thus the positron spectra for signal and background have different shapes, while the antiproton spectra have essentially the same shape and mainly differ in normalization.

The third issue concerns how the background is defined. The "background" can only be defined if one either has data in a region where there is known to be no signal, or if one has a theory of the background. There are two points. Some time ago reference [12] showed that solving the propagation equations allowed a rather large variation in the antiproton background normalization, about a factor of five for parameters that were consistent with other constraints

such as the Boron/Carbon ratio. This has also been emphasized by [12, 13]. Low energy data for antiprotons has existed for over a decade[14, 15, 16]. People proceeded by fitting the antiproton data and defining the fit as the background. Then they compared the PAMELA data with such backgrounds, and of course concluded there was no signal, because the signal had already been included in the background! If a dark matter annihilation contribution was included, it was double counted! As we show below, for entirely reasonable GALPROP parameters one can self-consistently compute the antiproton background, and with a wino annihilation signal it gives a good description of the data. Consequently the early experiments such as BESS and HEAT *did* detect dark matter via antiprotons.

There is another effect that has been neglected so far in most interpretations of the PAMELA and Fermi data. Dark matter annihilation is proportional to the square of the relic density. Because galaxies are built from smaller galaxies, and also because of normal random density fluctuations, the relic density throughout the relevant parts of the galaxy for a given observable will not be a flat  $0.3 \text{ GeV/cm}^3$ , but will vary. Since  $\langle \rho^2 \rangle - \langle \rho \rangle^2 \neq 0$ , density fluctuation effects must occur. Initial studies have been done by several authors[17, 18], who have established that the effects differ for positrons and for antiprotons, and are energy dependent, because the energy loss mechanisms are significantly different for positrons and antiprotons. While it is not clear yet how to calculate accurately the sizes and energy dependences of these effects, it is likely that assuming no effect is a less good approximation than initial approximate calculations of the effects. We include small effects we estimate semi-analytically and show results with and without them. Ultimately it will be very important to learn how to calculate these effects well and include them.

The positron data below  $10 - 15 \text{ GeV}$  is not consistent among experiments, and is not well described by models. This is assumed to be due to charge-dependent solar modulation effects and is being actively studied by experts in that area, and by the experimenters [19, 20]. We do not attempt to put in detailed corrections for this, but we do include the (non-charge-dependent) effects in the simulation. Results in general also depend on the profile of the dark matter in the galaxy, most importantly for gammas from the galactic center. We do not study this dependence much here since it does not much affect the positron and antiproton results, and we are computer-limited. We remark on it in context below.

The PAMELA experiment has reported deviations from expected astrophysics for positrons, and as we explained above, for antiprotons, below about  $100 \text{ GeV}$ . In this paper our goal is to demonstrate that a wino LSP is a strong candidate for explaining these deviations. We assume that possible astrophysical sources can be added to give a complete description of the data including Fermi (which light wino annihilation obviously cannot explain). We only parameterize the higher energy astrophysical part, and assume it can be accommodated by some combination of acceleration of the interstellar medium electrons by supernova remnant shock waves, pulsars, etc with a net  $e^+/e^-$  ratio of  $1/6$ . Once we do that we make a number of predictions for the positron ratio and antiprotons at energies above those already reported, for diffuse gammas and gammas from the galactic center, and for gamma fluxes from dwarf galaxies in our galactic halo. We check constraints from synchrotron radiation and "WMAP" haze. Our prediction for gammas assumes the source of higher energy  $e^+ + e^-$  does not also produce a significant flux of high energy gammas. So corrections may be needed here, but the gammas from wino annihilation will be an irreducible source.

We also do not criticize any other attempt to describe the data – in nearly all cases forthcoming PAMELA and Fermi data will favor one or another approach. Many are based on interesting ideas and models. While some predictions are very sensitive to propagation effects, others such as whether the positron ratio rises or falls above  $100 \text{ GeV}$  is not very sensitive to propagation and different models have very different predictions. We predict a fall or flattening (depending somewhat on the high energy astrophysical component), while most models predict a strong rise. While propagation uncertainties do not modify our qualitative predictions, it is clear that the presence of the rather hard contribution to the  $e^+ + e^-$  flux introduces uncertainty in our predictions, since it could affect the positron ratio at lower energies, and it might or might not contribute to antiproton and gamma fluxes. As described below, we simply parameterize it and we assume it only contributes to the electrons and positrons, and that it contains mostly electrons ( $e^+/e^- = 1/6$ ). This limits the quality of our predictions.

In the following we first describe our use of GALPROP in some detail, including some effects or constraints we incorporate. Then we show the data and a description of the data based on annihilation of  $180 \text{ GeV}$  dark matter winos plus cosmic ray backgrounds, with signal and backgrounds computed in a consistent manner. What we show is not a fit to data but merely educated guesses since the computing time for a full parameter scan is still prohibitive for us. As shown in Table I below, we vary eight GALPROP parameters and some others, and all of them affect the interpretation. We have established that comparable descriptions of the data can be obtained for different GALPROP parameters from those we show since there are degeneracies. We emphasize that our goal is to show that the wino LSP in the mass range of order  $200 \text{ GeV}$  is a good candidate for the dark matter of the universe, including theoretical and experimental information as well as it is possible today. Even though much is not known about the propagation of the electrons, positrons, antiprotons and gammas, quite a lot *is* known. Then we describe the contribution we arbitrarily assume for the higher energy electrons and positrons. We will report on studies of the GALPROP parameter degeneracies and the wino mass later, assuming our predictions for the positron and antiproton higher energy data are correct.

After that we turn to presenting the data and the descriptions. We do that for one mass and one set of propagation parameters, and one dark matter profile (NFW). Descriptions and predictions for higher energies are shown for the PAMELA positron excess, the PAMELA antiproton excess, the  $e^+ + e^-$  sum, the diffuse gammas, the gammas from the galactic center, dwarf galaxies, and checks such as the Boron/Carbon ratio. Finally we present conclusions and a list of tests of the wino LSP model. Definitive tests of this approach will also occur at the LHC; we will present those elsewhere. When future data is reported we will post updated graphs at <http://wino.physics.lsa.umich.edu>.

## II. GALPROP PARAMETERS

We use GALPROP v50.1p[9] to simulate the propagation of both cosmic rays and dark matter annihilation products in the galaxy in a consistent way. The rates and spectrum for both will change if the propagation parameters change. The propagation process is described by the propagation equation for the particle density  $\psi$ :

$$\begin{aligned} \frac{\partial \psi}{\partial t} = & q(\vec{r}, p) + \vec{\nabla} \cdot (D_{xx} \vec{\nabla} \psi - \vec{V} \psi) + \frac{\partial}{\partial p} p^2 D_{pp} \frac{\partial}{\partial p} \frac{1}{p^2} \psi \\ & - \frac{\partial}{\partial p} \left[ \dot{p} \psi - \frac{p}{3} (\vec{\nabla} \cdot \vec{V}) \psi \right] - \frac{1}{\tau_f} \psi - \frac{1}{\tau_r} \psi \end{aligned} \quad (1)$$

where  $D_{xx}$  is the diffusion constant which is determined by:

$$D_{xx} = \beta D_{0xx} \left( \frac{\mathcal{R}}{\mathcal{R}_0} \right)^\delta \quad (2)$$

where  $\beta$  is the velocity of the particle,  $\mathcal{R}$  is the particle rigidity, and  $\mathcal{R}_0$  is the reference rigidity which is taken to be 4 GV in all the simulations. In order to consider the propagation of the dark matter signals in the same framework, the official GALPROP code is modified to accept the dark matter injection spectrum calculated using PYTHIA via DarkSUSY 5.0.4[10]. The parameters used in this paper are based on the conventional model with constant Xco-factor provide in GALPROP source code (galdef\_50p\_599278). In general we vary the parameters  $D_{xx}$ ,  $\delta$ , the half height of the diffusion zone  $z_h$ , the primary electron injection index  $\gamma_0$ , the normalization of the primary electron flux  $N_{e^-}$ , the scaling factor for inverse Compton scattering, the convection velocity  $V_c$ , and the Alfvén velocity  $V_a$ . We survey ranges of these parameters (but do not fit data or scan parameters because of computing limitations) in order to learn if a combination of conventional cosmic ray physics plus dark matter annihilation can give a reasonable description of the PAMELA and Fermi data within certain constraints such as the B/C ratio described further below.

We find a set of parameters that give a good description of the data, and those are used in the figures below except when stated otherwise. The half height of the diffusion zone  $z_h = 2$  kpc. The diffusion coefficient is  $D_{0xx} = 2.5 \times 10^{28} \text{ cm}^2 \text{ s}^{-1}$ ,  $\delta = 0.5$ . We also assume a softer primary electron injection spectrum by setting the injection index  $\gamma_0$  for primary electrons between 4 GeV to  $10^6$  GeV to 2.6. Also the primary electron flux is normalized to  $N_{e^-} = 2.88 \times 10^{-10} \text{ cm}^{-2} \text{ sr}^{-1} \text{ s}^{-1} \text{ MeV}^{-1}$  at 34.5 GeV. The scaling factors for inverse Compton (ISRF factor) are adjusted to 0.5, which is approximately equivalent to setting  $\tau = 2 \times 10^{16} \text{ s}$  in the energy loss rate formula for electron  $b(\varepsilon)_{e^\pm} = \frac{1}{7} \varepsilon^2$ . The convection velocity is  $V_c = 5 \text{ km s}^{-1} \text{ kpc}^{-1}$ , and the Alfvén speed which determines the reacceleration process is  $V_a = 31 \text{ km s}^{-1}$ . The summary of the parameters we are using can be found in Table I. Other parameters not mentioned here are the same as galdef\_50p\_599278.

As described in the introduction, the dark matter we focus on is the theoretically well-motivated case of a pure wino LSP, which annihilates to  $W$ 's:  $\widetilde{W} + \widetilde{W} \rightarrow W^+ + W^-$ . The dark matter injection parameters are then completely determined by the wino mass and  $W^\pm$  decays.

## III. SOLAR MODULATION

The effect of solar modulation is estimated by the Force-Field approximation [21], The flux observed at Earth's orbit  $J_E(\varepsilon)$  is related to the flux in the interstellar flux by the following relation:

$$J_E(\varepsilon) = \frac{\varepsilon^2 - m^2}{\varepsilon_\infty^2 - m^2} J_\infty(\varepsilon_\infty) \quad (3)$$

GALPROP Parameters	
$D_{xx0}$ ( $\text{cm}^2\text{s}^{-1}$ )	$2.5 \times 10^{28}$
$\delta$	0.5
$\mathcal{R}_0$ (GV)	4
$z_h$ (kpc)	2
$\gamma_0$	2.6
$N_{e^-}$ ( $\text{cm}^{-2}\text{s}^{-1}\text{sr}^{-1}\text{MeV}^{-1}$ )	$2.88 \times 10^{-10}$
$V_c$ ( $\text{kms}^{-1}\text{kpc}^{-1}$ )	5
$V_a$ ( $\text{kms}^{-1}$ )	31
ISRF factors (optical, FIR, CMB)	0.5, 0.5, 0.5
Solar Modulation Parameters	
$\phi$ (MV)	500
$p_c$ (GeV)	1
Astrophysical Flux Parameters	
$a$	1.0
$b$	1.8
$z_0$ (kpc)	0.2
$\gamma$	1.5
$M$ (GeV)	950
Density Fluctuation Factor Parameters	
$B_c$	2.5
$f$	0.5

TABLE I: The parameters used for simulation. The physical meaning of these parameters is described in the text.

where  $\varepsilon_\infty$  is the energy of the corresponding interstellar flux, which is determined by:

$$\varepsilon_\infty = \begin{cases} p \log\left(\frac{p_c + \varepsilon_c}{p + \varepsilon}\right) + \varepsilon + \Phi & \varepsilon < \varepsilon_c \\ \varepsilon + \Phi & \varepsilon \geq \varepsilon_c \end{cases} \quad (4)$$

$\Phi$  is the modulation energy shift which can be calculated from the modulation potential  $\Phi = |Z|e\phi$ . In our simulation the modulation potential  $\phi$  is 500 MV, the reference momentum  $p_c$  is 1 GeV. Only the solar modulation effect for electron/positron and antiproton/proton is considered in this work. These effects do not include charge dependent solar modulation, which is under study [19, 20]

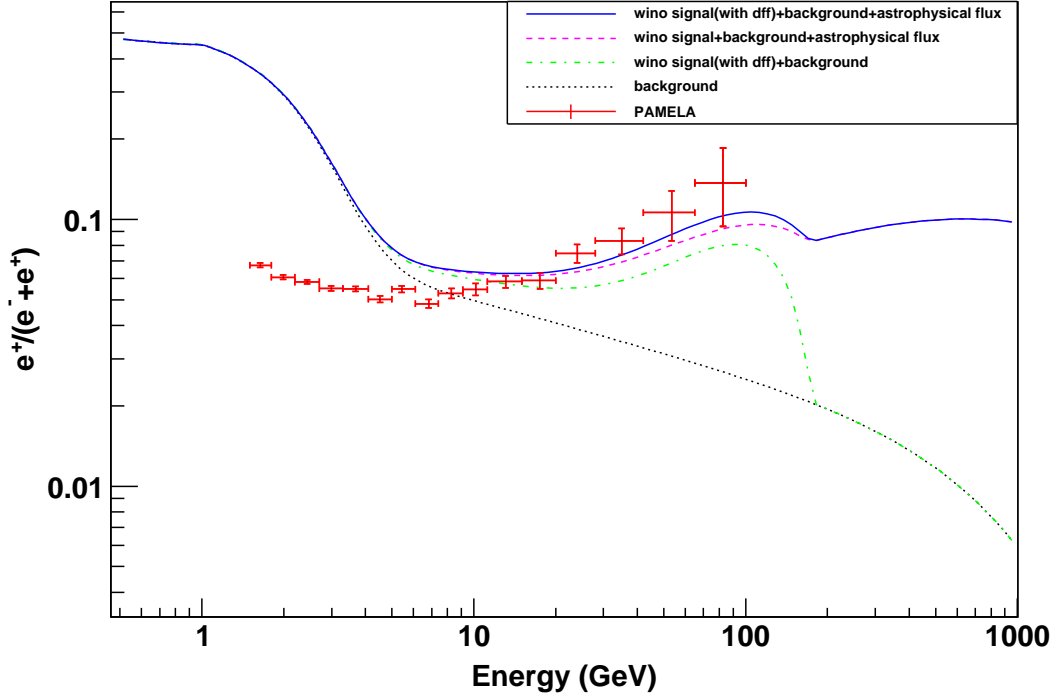


FIG. 1: The positron flux ratio, generated with the parameters described in the text and Table I with a  $M_{\tilde{W}} = 180$  GeV wino. The solid line is the ratio of the total positron flux, which includes the positrons from the wino annihilation, the density fluctuation factor, the astrophysical flux and the conventional astrophysics background to positrons plus electrons. The dash line has the same components but without the density fluctuation factor. The dash-dot line contains just the wino annihilation and the conventional astrophysics background, and the dot line is the ratio of the secondary positrons only. The data are from [22], Our analysis assumes the reported normalization of the Fermi and PAMELA data. If those change it will affect the higher energy extrapolation here. Note that the predicted positron fraction does not continue to rise. At the PAMELA meeting in Rome [20] data was reported with the four higher energy points about 10% lower than shown here, but we do not show that data since it has not yet been published.

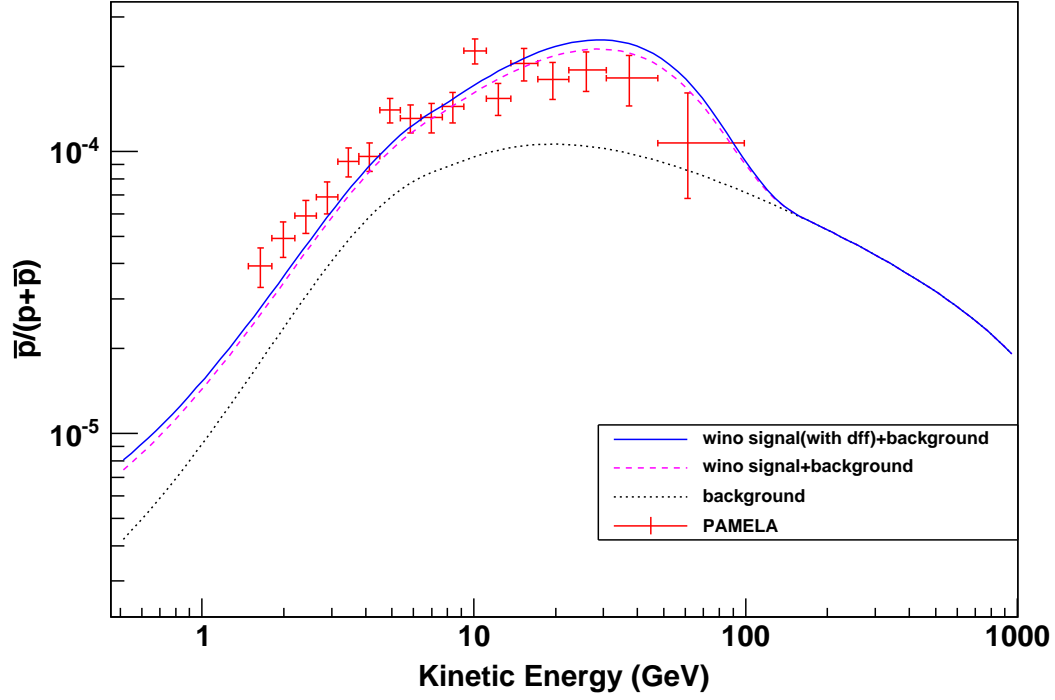


FIG. 2: The antiproton flux ratio. The solid line is the ratio of the total antiproton flux, which include the antiproton from wino annihilation, and conventional astrophysics background, the dash line has the same components but without the density fluctuation factor, the dot line is astrophysics background only. The data are from PAMELA [23]. At the PAMELA meeting in Rome[20], data was reported with the last bin increased by 70%, and a bin up to 185 GeV with three events, but we do not show the data since it is not published. Note the signal is larger than the background down to very low energies.

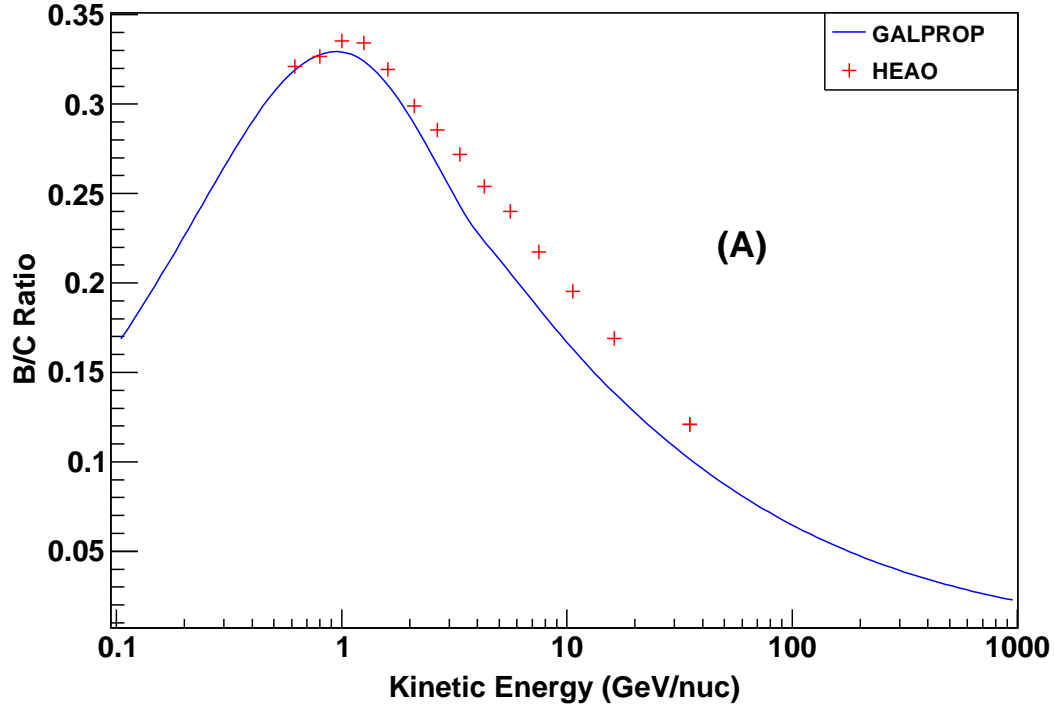


FIG. 3: The Boron to Carbon ratio with our standard parameters, solar modulation effect is not included, The data are from [24].

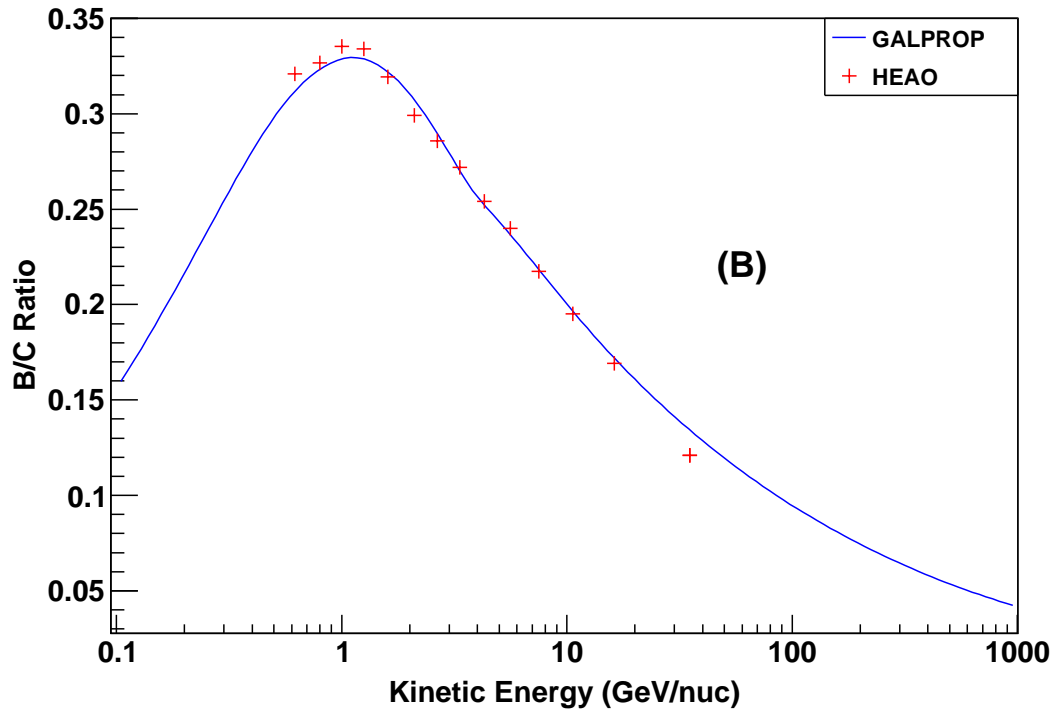


FIG. 3: The Boron to Carbon ratio with one parameter different ( $\delta$  changes from 0.5 to 0.4). This illustrates that the Boron to Carbon ratio is very sensitive the diffusion parameters. The data are from [24].



#### IV. ASTROPHYSICAL FLUX

It is obvious that a 180 GeV wino alone cannot explain Fermi data and PAMELA data at the same time. There must be some extra flux responsible for the high energy signals. In order to estimate the high energy ( $> 200$  GeV) electrons/positrons flux, we consider a simple model for extra flux which is suggested by interstellar medium electrons accelerated by supernova remnants and shock waves, or by pulsar spectra models. The basic setup we use is similar to Zhang and Cheng[25]. For a recent review of pulsar models, see Profumo[26]. The spatial distribution of the sources is:

$$\rho(r) = N \left( \frac{r}{r_{\odot}} \right)^a e^{-\frac{b(r-r_{\odot})}{r_{\odot}}} e^{-\frac{z}{z_0}} \quad (5)$$

where  $N$  is the overall normalization constant,  $z_0 = 0.2$  kpc,  $r_{\odot} = 8.5$  kpc,  $a = 1.0$  and  $b = 1.8$ .

The energy dependence of the injection spectrum is:

$$\frac{dN_{e^{\pm}}}{dE} = N' E^{-\gamma} e^{-\frac{E}{M}} \quad (6)$$

where  $N'$  is another normalization constant, which can be absorbed into  $N$ ,  $\gamma = 1.5$  and  $M = 950$  GeV. In order to fit PAMELA and Fermi data, we made an ad hoc assumption that the ratio of positron and electron in the unknown extra flux is 1 : 6. The high energy positrons/electrons are then propagated by GALPROP, and the resulting flux is normalized to fit the Fermi data by requiring the extra electron flux at 275.5 GeV to be  $3.0 \times 10^{-13} \text{ cm}^{-2} \text{ sr}^{-1} \text{ s}^{-1} \text{ MeV}^{-1}$

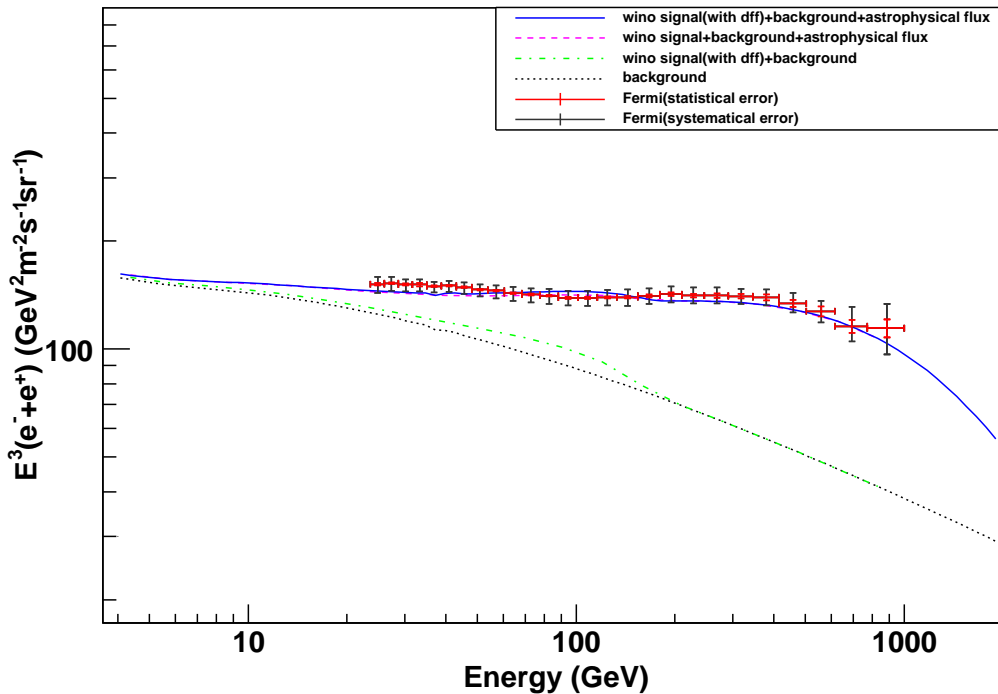


FIG. 4: The absolute flux of  $e^+ + e^-$ , The solid line is the sum of electron and positron from the wino annihilation, the density fluctuation factor, our assumed extra flux, and conventional astrophysics background, the dash line has the same components but without the density fluctuation factor. The dash-dot line contains wino annihilation and astrophysics background, and the dot line is the conventional astrophysics background only. See comments in Figure 1. The data are from [27].

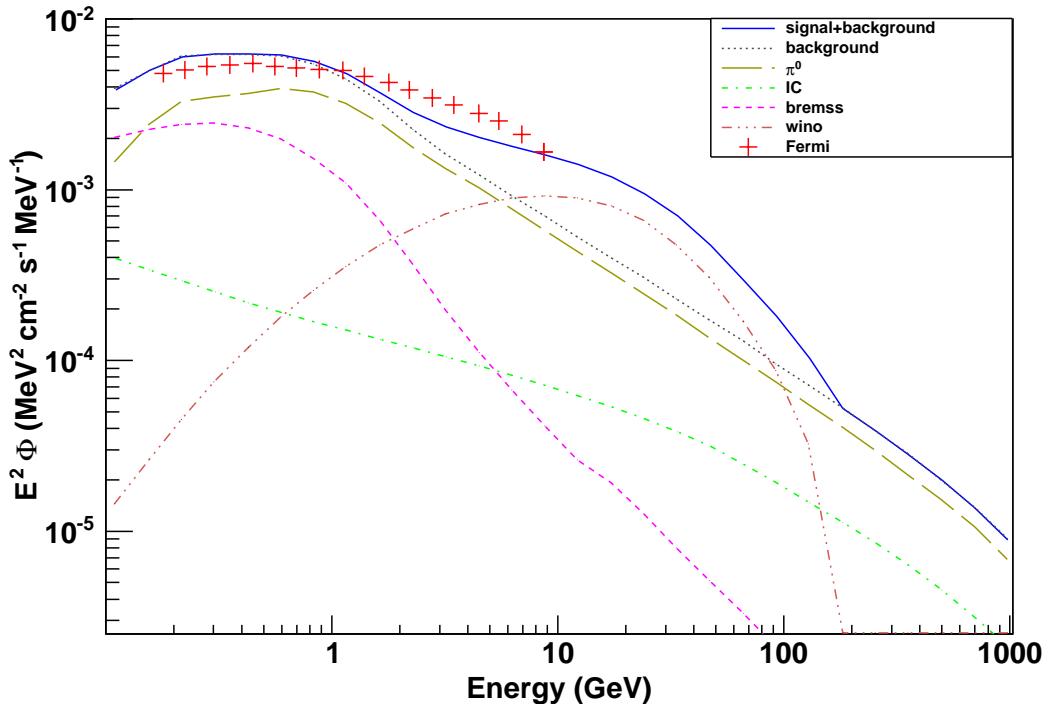


FIG. 5: Different components of the diffusive gamma ray emission averaged over  $10^\circ \leq |b| \leq 20^\circ$  region, The gamma ray emission is integrated over a spherical halo with radius  $r = 20$  kpc. All parameters as in Table I, and wino mass  $M_{\tilde{W}} = 180$  GeV. The solid line is the total flux, the dot line is the total background, the long dash line is the flux from  $\pi^0$  decay, the dash-dot line is the flux from inverse Compton, the dash line is the flux from bremsstrahlung, and the dash-dot-dot line is the flux from wino annihilation. All parameters as in Table I, and wino mass  $M_{\tilde{W}} = 180$  GeV. The data are from [28].

## V. DENSITY FLUCTUATION FACTOR

The results from N-body simulations [29], and an understanding of how galaxies formed, indicate that it is inevitable for the dark matter halo of our galaxy to have substructures. The existence of these substructures would change the predictions of the cosmic ray fluxes, particularly for dark matter annihilation. Even without substructures, it is clear that the density of dark matter will not be absolutely flat, but will fluctuate around an average value. Both of these effects require the flux from dark matter annihilation, which is sensitive to the square of the dark matter density, to show density fluctuation effects. As emphasized by Lavallo and collaborators [17, 18], the effects of these substructures are different for positrons and antiproton, and must also be energy dependent. The details of these effects depend on the spatial and mass distribution of these substructures. Here<sup>1</sup> we use a very simple model to estimate the effects: Assuming all the substructures share the same mass and density, and the spatial number density of the substructures is proportional to the density profile of the smooth distribution of dark matter halo.

With these assumptions, the density fluctuation factor can be calculated with:

$$D(E) = (1 - f)^2 + f B_c \frac{\mathcal{I}_1}{\mathcal{I}_2} \quad (7)$$

where  $f$  is the mass fraction of the substructures in the dark matter halo,  $B_c$  is the intrinsic density increase of the

<sup>1</sup> The analysis of this section was carried out in collaboration with Cheng Peng.

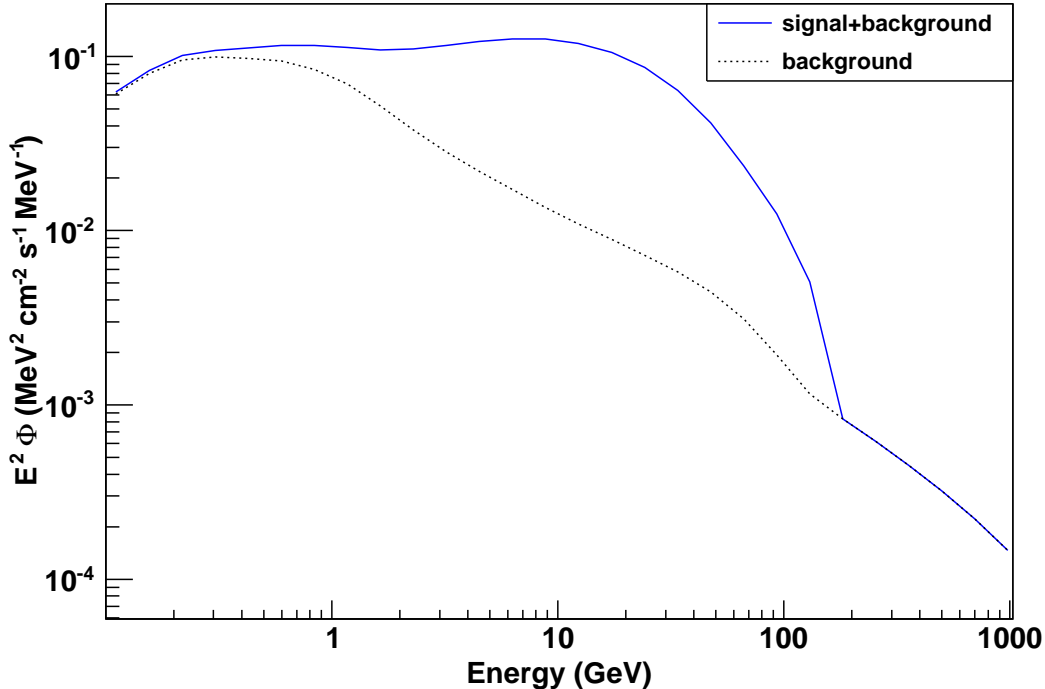


FIG. 6: Gamma ray emission from the galactic center, the flux is averaged over  $|l| \leq 0.5^\circ$ ,  $|b| \leq 0.5^\circ$ . All parameters as in Table I, and wino mass  $M_{\tilde{W}} = 180$  GeV.

substructures or fluctuations, and  $\mathcal{I}_n$  is determined by

$$\mathcal{I}_n = \int_{\text{DM halo}} G(x, E) \left\{ \frac{\rho_s(x)}{\rho_0} \right\}^n d^3x \quad (8)$$

where  $G(x, E)$  is the Green's function of the propagating particle.

We assume  $f = 0.5$  and  $B_c = 2.5$ . Only the density fluctuations of positron and antiproton are considered. The electron/positron Green's function from Baltz and Edsjö[30] and the fast formulae for antiproton Green's function from Maurin, Taillet and Combet[31] are used to evaluate the integral. With these assumptions we find the effects are small. We included them for completeness. Theory curves including them are labeled “dff” (for “density fluctuation factors”) in the figures.

## VI. DWARF GALAXIES

Dwarf spheroidal satellite galaxies are unique targets for indirect detection of dark matter[32]. Most of them are believed to be dark matter dominated objects and some of them are located at high Galactic latitudes, which reduces the diffusive gamma background. But the dark matter density profiles of these dwarf galaxies are hard to determine, which gives large uncertainties in the predictions[33, 34, 35].

We calculate the gamma ray flux from wino annihilation in these dwarf galaxies following Essig, Sehgal and Strigari[35]. The formula for the gamma ray flux from annihilating dark matter in a dark matter halo is

$$\frac{dN_\gamma}{dAdt} = \frac{1}{8\pi} \mathcal{L}_{\text{ann}} \frac{\langle \sigma v \rangle}{M_{\tilde{W}}^2} \int_{E_{\text{th}}}^{E_{\text{max}}} \frac{dN_\gamma}{dE_\gamma} dE_\gamma \quad (9)$$

where in our model the annihilation cross-section  $\langle \sigma v \rangle = 2.50 \times 10^{-24} \text{ cm}^3 \text{ s}^{-1}$ , and the wino mass  $M_{\tilde{W}}$  is set at 177.5 GeV (it is not exactly 180 GeV because the soft SUSY breaking terms changed the spectrum a little bit). We take the threshold energy  $E_{\text{th}} = 100$  MeV, the integration  $\int_{E_{\text{th}}}^{E_{\text{max}}} \frac{dN_\gamma}{dE_\gamma} dE_\gamma = 27.14$ .  $\mathcal{L}_{\text{ann}} = \int_0^{\Delta\Omega} \left\{ \int_{\text{LOS}} \rho^2(r) ds \right\} d\Omega$ ,

Dwarf Galaxies	$\mathcal{L}_{\text{ann}}$ $\log_{10} [\text{GeV}^2 \text{c}^{-4} \text{cm}^{-5}]$	Flux ( $E_{\text{th}} = 100 \text{ MeV}$ ) $10^{-9} \text{cm}^{-2} \text{s}^{-1}$
Sagittarius	$19.35 \pm 1.66$	1.9 (0.042, 88)
Draco	$18.63 \pm 0.60$	0.36 (0.092, 1.5)
Ursa Minor	$18.79 \pm 1.26$	0.53 (0.029, 9.6)
Willman 1	$19.55 \pm 0.98$	3.0 (0.32, 29)
Segue 1	$20.17 \pm 1.44$	13 (0.46, 350)

TABLE II: The wino LSP prediction of gamma ray flux from some dwarf galaxies, based on the calculation of  $\mathcal{L}_{\text{ann}}$  in [35]. The three numbers in the flux column are the central value and the maximum and minimum value corresponding to the  $\mathcal{L}_{\text{ann}}$  result. The results are consistent with the recently reported preliminary flux upper limits for 3-month Fermi LAT data [36], and suggest signals may be observed with Fermi LAT in the near future.

which only depends on the properties of the dark matter halo and the solid angle over which it is observed, can be found in Table 1 of [35]. The results of our estimate of the gamma ray fluxes from several dwarf galaxies is presented in Table II. Although limits are reported for some dwarf galaxies [36] we cannot directly compare our predictions with those limits since they are somewhat dependent on the analysis. We estimated the corresponding constraints for the wino LSP by scaling the cross section upper bound for the  $b\bar{b}$  final state provided by [36] to the corresponding wino LSP cross section upper bound which gives the same amount of gamma ray flux. Different dSph give upper bounds on the cross section ranging from  $1.6 \times 10^{-24} \text{cm}^3 \text{s}^{-1}$  to  $3.6 \times 10^{-23} \text{cm}^3 \text{s}^{-1}$ , with Willman1 giving the most stringent constraint. As shown in the Table, after the uncertainty of the halo density profile is taken into account, the wino LSP predictions are allowed by the limits. At the same time, the predictions are large enough to anticipate seeing a signal soon.

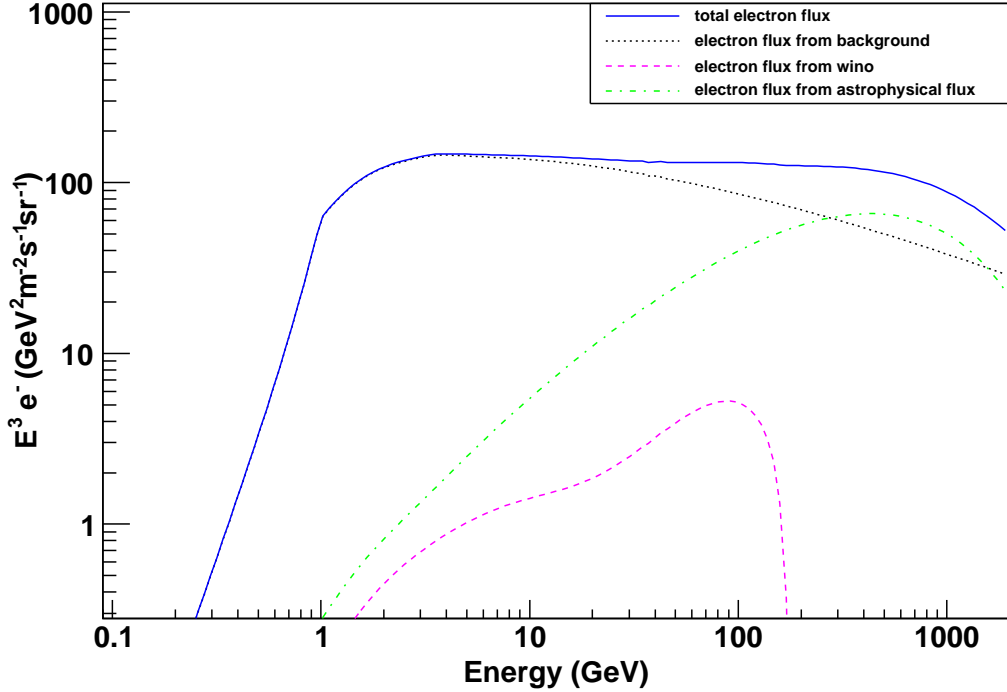


FIG. 7: The absolute flux of  $e^-$ , the solid line is the sum of all the components, the dot line is the conventional astrophysics background, the dash line is the wino annihilation signal, and the dash-dot line is the contribution from the extra flux.

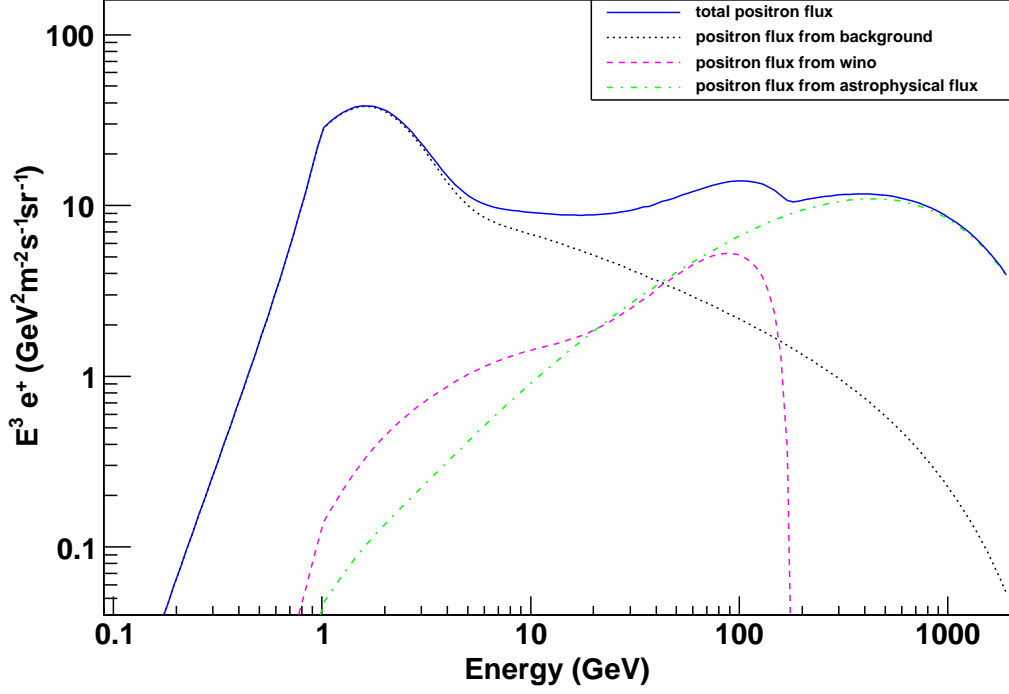


FIG. 8: The absolute flux of  $e^+$ , the solid line is the sum of all the components, the dot line is the conventional astrophysics background, the dash line is the wino annihilation signal, and the dash-dot line is the contribution from the extra flux.

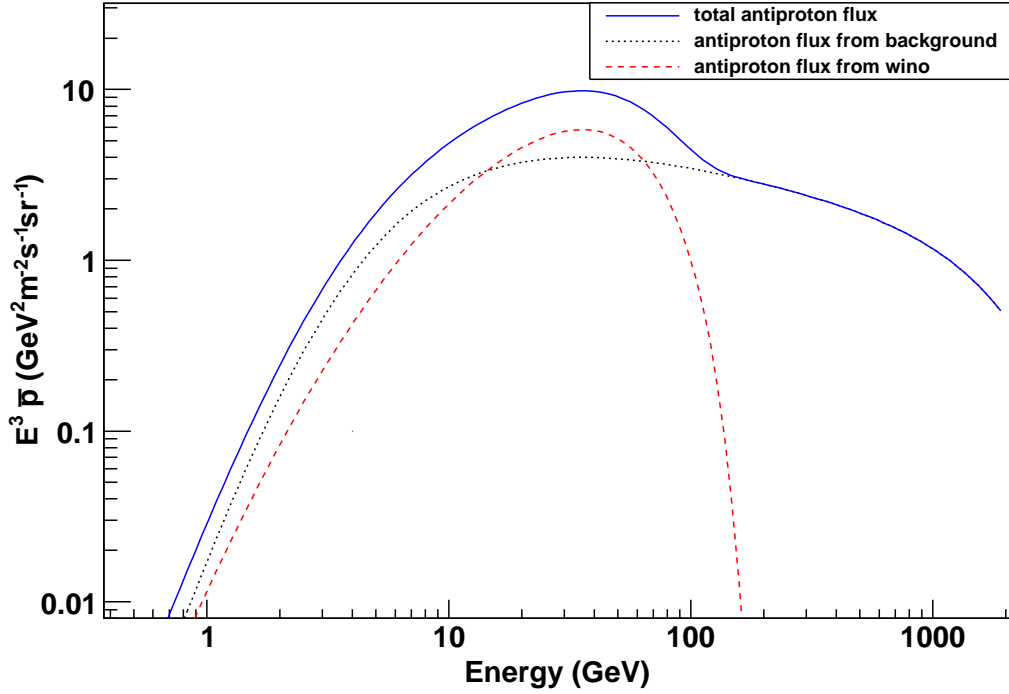


FIG. 9: The absolute flux of  $\bar{p}$ , the solid line is the sum of all the components, the dot line is the conventional astrophysics background, and the dash line is the wino annihilation signal.

## VII. LHC

The LHC phenomenology of the wino LSP is fairly well studied because it originally occurred in the anomaly mediated context[4, 7], The production rates are large,  $\sim 10$  pb for charginos and neutralinos. The triggers and signatures are difficult since the chargino and LSP are approximately degenerate[37, 38, 39, 40, 41],. Probably the main trigger will be the associated gluino production and decay. Gluino masses in models range from a few to about 10 times the LSP mass, all within the LHC range. We will report on these topics later.

## VIII. SUMMARY OF TESTS AND COMMENTS

There will be definitive tests of the existence of a wino LSP with the mass range we consider at the LHC. We summarize here tests that will occur from astrophysical data and analysis soon. At this stage we cannot make strong statements about direct detection, since pure winos have small scattering cross section. The rates are very sensitive to mixtures of binos and higgsinos, but the present data plus the propagation uncertainties do not determine the mixtures very well. Also the contribution from  $\chi\chi \rightarrow \gamma\gamma$  and  $\chi\chi \rightarrow Z\gamma$  is not included in this study, since the cross sections, calculated with DarkSUSY using the analytical formulas given in [42], are relatively small ( $2.25 \times 10^{-27} \text{cm}^3 \text{s}^{-1}$  for  $\gamma\gamma$  and  $1.36 \times 10^{-26} \text{cm}^3 \text{s}^{-1}$  for  $Z\gamma$  respectively).

Astrophysical tests includes the following. For some the presence of high energy astrophysical contribution needs to be kept in mind. When future data is reported we will post updated graphs at <http://wino.physics.lsa.umich.edu>.

1. Turnover or flattening of the positron ratio and the positron absolute flux with increasing energy. (Figure 1, 8).
2. The rise in the positron ratio is not due to a decrease in the electron flux, which will not decrease faster in the region from 10 - 200 GeV. (Figure 7).
3. The  $\bar{p}$  rate will turn over with increasing energy. (Figure 2, 9).
4. There will be an observable excess in the region below 200 GeV in the diffusive gamma spectrum, by a factor of order 3 - 4 from wino annihilation (Figure 5)
5. There will be an increase in gammas from the galactic center below 200 GeV from wino annihilation, almost an order of magnitude (Figure 6)
6. Effects on synchrotron radiation (WMAP haze)[43, 44] and recombination[45, 46, 47] need further detailed study. Wino annihilation is consistent with the current experimental constraints[47, 48, 49], though barely if all their assumptions are accepted. This may mean the wino annihilation is an explanation. Planck data will provide a significant test here.
7. Effects from wino annihilation for dwarf galaxies are probably observable (Table II)

If wino-like dark matter annihilation is indeed being observed, the implications are remarkable. We are not only learning what constitutes the dark matter, it is also the discovery of supersymmetry, and learning that the universe has a non-thermal cosmological history that can be studied. These implications in turn favor certain underlying theories.

## IX. ACKNOWLEDGEMENTS

We are grateful for discussions with Bobby Acharya, Nima Arkani-Hamed, Lars Bergström, Elliott Bloom, Mirko Boezio, Joachim Edsjö, Rouven Essig, Phill Grajek, Emiliano Macchiutti, Patrick Meade, Aldo Morselli, Igor Moskolenko, Michele Papucci, Cheng Peng, Piergiorgio Picozza, Tomer Volansky, Liantao Wang, Neal Weiner, and particularly Aaron Pierce who also collaborated on parts of the research. S.W. would like to thank KITP, Perimeter Institute, and the University of Texas - Austin for hospitality, and also U of T - Austin for financial support under National Science Foundation Grant No. PHY-0455649.

---

[1] M. Kamionkowski and M. S. Turner, "Thermal relics: Do we know their abundances?," *Phys. Rev.* **D42** (1990) 3310-3320.

- [2] D. J. H. Chung, E. W. Kolb, and A. Riotto, “Nonthermal supermassive dark matter,” *Phys. Rev. Lett.* **81** (1998) 4048–4051, [arXiv:hep-ph/9805473](#).
- [3] G. F. Giudice, E. W. Kolb, and A. Riotto, “Largest temperature of the radiation era and its cosmological implications,” *Phys. Rev.* **D64** (2001) 023508, [arXiv:hep-ph/0005123](#).
- [4] T. Moroi and L. Randall, “Wino cold dark matter from anomaly-mediated SUSY breaking,” *Nucl. Phys.* **B570** (2000) 455–472, [arXiv:hep-ph/9906527](#).
- [5] B. S. Acharya *et al.*, “Non-thermal Dark Matter and the Moduli Problem in String Frameworks,” *JHEP* **06** (2008) 064, [arXiv:0804.0863 \[hep-ph\]](#).
- [6] G. Kane and S. Watson, “Dark Matter and LHC: What is the Connection?,” *Mod. Phys. Lett.* **A23** (2008) 2103–2123, [arXiv:0807.2244 \[hep-ph\]](#).
- [7] L. Randall and R. Sundrum, “Out of this world supersymmetry breaking,” *Nucl. Phys.* **B557** (1999) 79–118, [arXiv:hep-th/9810155](#).
- [8] P. Langacker, G. Paz, L.-T. Wang, and I. Yavin, “Z'-mediated Supersymmetry Breaking,” *Phys. Rev. Lett.* **100** (2008) 041802, [arXiv:0710.1632 \[hep-ph\]](#).
- [9] A. W. Strong and I. V. Moskalenko, “Propagation of cosmic-ray nucleons in the Galaxy,” *Astrophys. J.* **509** (1998) 212–228, [arXiv:astro-ph/9807150](#).
- [10] P. Gondolo, J. Edsjö, P. Ullio, L. Bergström, M. Schelke, and E. A. Baltz, “DarkSUSY: Computing supersymmetric dark matter properties numerically,” *JCAP* **0407** (2004) 008, [arXiv:astro-ph/0406204](#).
- [11] P. Gondolo, J. Edsjö, P. Ullio, L. Bergström, M. Schelke, E. A. Baltz, T. Bringmann, and G. Duda. <http://www.physto.se/~edsjo/darksusy>.
- [12] F. Donato, N. Fornengo, D. Maurin, and P. Salati, “Antiprotons in cosmic rays from neutralino annihilation,” *Phys. Rev.* **D69** (2004) 063501, [arXiv:astro-ph/0306207](#).
- [13] L. Bergstrom, J. Edsjo, M. Gustafsson, and P. Salati, “Is the dark matter interpretation of the EGRET gamma excess compatible with antiproton measurements?,” *JCAP* **0605** (2006) 006, [arXiv:astro-ph/0602632](#).
- [14] BESS Collaboration, S. Orito *et al.*, “Precision measurement of cosmic-ray antiproton spectrum,” *Phys. Rev. Lett.* **84** (2000) 1078–1081, [arXiv:astro-ph/9906426](#).
- [15] BESS Collaboration, T. Maeno *et al.*, “Successive measurements of cosmic-ray antiproton spectrum in a positive phase of the solar cycle,” *Astropart. Phys.* **16** (2001) 121–128, [arXiv:astro-ph/0010381](#).
- [16] Y. Asaoka *et al.*, “Measurements of cosmic-ray low-energy antiproton and proton spectra in a transient period of the solar field reversal,” *Phys. Rev. Lett.* **88** (2002) 051101, [arXiv:astro-ph/0109007](#).
- [17] J. Lavalle, J. Pochon, P. Salati, and R. Taillet, “Clumpiness of dark matter and positron annihilation signal: Computing the odds of the galactic lottery,” [arXiv:astro-ph/0603796](#).
- [18] J. Lavalle, Q. Yuan, D. Maurin, and X. J. Bi, “Full Calculation of Clumpiness Boost factors for Antimatter Cosmic Rays in the light of  $\Lambda$ CDM N-body simulation results,” [arXiv:0709.3634 \[astro-ph\]](#).
- [19] J. M. Clem, D. P. Clements, J. Esposito, P. Evenson, D. Huber, J. L’Heureux, P. Meyer, and C. Constantin, “Solar Modulation of Cosmic Electrons,” *Astrophysical Journal* **464** (June, 1996) 507–+.
- [20] See recent talks at PAMELA workshop. <http://pamela.roma2.infn.it/workshop09/index.php/scientific-program>.
- [21] L. J. Gleeson and W. I. Axford, “Cosmic Rays in the Interplanetary Medium,” *Astrophysical Journal* **149** (Sept., 1967) L115–L118.
- [22] PAMELA Collaboration, O. Adriani *et al.*, “An anomalous positron abundance in cosmic rays with energies 1.5–100 GeV,” *Nature* **458** (2009) 607–609, [arXiv:0810.4995 \[astro-ph\]](#).
- [23] O. Adriani *et al.*, “A new measurement of the antiproton-to-proton flux ratio up to 100 GeV in the cosmic radiation,” *Phys. Rev. Lett.* **102** (2009) 051101, [arXiv:0810.4994 \[astro-ph\]](#).
- [24] J. J. Engelmann, P. Ferrando, A. Soutoul, P. Goret, and E. Juliusson, “Charge composition and energy spectra of cosmic-ray nuclei for elements from Be to Ni - Results from HEAO-3-C2,” *Astronomy and Astrophysics* **233** (July, 1990) 96–111.
- [25] L. Zhang and K. S. Cheng, “Cosmic-ray positrons from mature gamma-ray pulsars,” *Astronomy and Astrophysics* **368** (Mar., 2001) 1063–1070.
- [26] S. Profumo, “Dissecting Pamela (and ATIC) with Occam’s Razor: existing, well-known Pulsars naturally account for the ‘anomalous’ Cosmic-Ray Electron and Positron Data,” [arXiv:0812.4457 \[astro-ph\]](#).
- [27] The Fermi LAT Collaboration, A. A. Abdo *et al.*, “Measurement of the Cosmic Ray e+ plus e- spectrum from 20 GeV to 1 TeV with the Fermi Large Area Telescope,” [arXiv:0905.0025 \[astro-ph.HE\]](#).
- [28] A. Morselli, “Search for Dark Matter in the Fermi era,” *The LHC and Dark Matter Workshop at MCTP, January 6-10, 2009* (2009) .
- [29] J. Diemand, B. Moore, and J. Stadel, “Earth-mass dark-matter haloes as the first structures in the early universe,” *Nature*. **433** (2005) 389–391, [arXiv:astro-ph/0501589](#).
- [30] E. A. Baltz and J. Edsjo, “Positron Propagation and Fluxes from Neutralino Annihilation in the Halo,” *Phys. Rev.* **D59** (1998) 023511, [arXiv:astro-ph/9808243](#).
- [31] D. Maurin, R. Taillet, and C. Combet, “Approximate formulae for exotic GCR anti-p and anti-d: Fluxes and astrophysical uncertainties,” [arXiv:astro-ph/0609522](#).
- [32] N. W. Evans, F. Ferrer, and S. Sarkar, “A ‘Baedeker’ for the dark matter annihilation signal,” *Phys. Rev.* **D69** (2004) 123501, [arXiv:astro-ph/0311145](#).
- [33] L. E. Strigari, S. M. Koushiappas, J. S. Bullock, and M. Kaplinghat, “Precise constraints on the dark matter content of Milky Way dwarf galaxies for gamma-ray experiments,” *Phys. Rev.* **D75** (2007) 083526, [arXiv:astro-ph/0611925](#).

- [34] L. E. Strigari *et al.*, “The Most Dark Matter Dominated Galaxies: Predicted Gamma-ray Signals from the Faintest Milky Way Dwarfs,” [arXiv:0709.1510](#) [[astro-ph](#)].
- [35] R. Essig, N. Sehgal, and L. E. Strigari, “Bounds on Cross-sections and Lifetimes for Dark Matter Annihilation and Decay into Charged Leptons from Gamma-ray Observations of Dwarf Galaxies,” [arXiv:0902.4750](#) [[hep-ph](#)].
- [36] B. Winer, “Searching for Dark Matter with the Fermi Gamma-Ray Space Telescope,” *SUSY09 Plenary Talk* (2009) .
- [37] J. L. Feng, T. Moroi, L. Randall, M. Strassler, and S.-f. Su, “Discovering supersymmetry at the Tevatron in Wino LSP scenarios,” *Phys. Rev. Lett.* **83** (1999) 1731–1734, [arXiv:hep-ph/9904250](#).
- [38] T. Gherghetta, G. F. Giudice, and J. D. Wells, “Phenomenological consequences of supersymmetry with anomaly-induced masses,” *Nucl. Phys.* **B559** (1999) 27–47, [arXiv:hep-ph/9904378](#).
- [39] M. Ibe, T. Moroi, and T. T. Yanagida, “Possible signals of Wino LSP at the Large Hadron Collider,” *Phys. Lett.* **B644** (2007) 355–360, [arXiv:hep-ph/0610277](#).
- [40] S. Asai, T. Moroi, and T. T. Yanagida, “Test of Anomaly Mediation at the LHC,” *Phys. Lett.* **B664** (2008) 185–189, [arXiv:0802.3725](#) [[hep-ph](#)].
- [41] B. S. Acharya, K. Bobkov, G. L. Kane, J. Shao, and P. Kumar, “The  $G_2$ -MSSM - An  $M$  Theory motivated model of Particle Physics,” *Phys. Rev.* **D78** (2008) 065038, [arXiv:0801.0478](#) [[hep-ph](#)].
- [42] L. Bergstrom and P. Ullio, “Full one-loop calculation of neutralino annihilation into two photons,” *Nucl. Phys.* **B504** (1997) 27–44, [arXiv:hep-ph/9706232](#).
- [43] D. Hooper, “Constraining Supersymmetric Dark Matter With Synchrotron Measurements,” *Phys. Rev.* **D77** (2008) 123523, [arXiv:0801.4378](#) [[hep-ph](#)].
- [44] D. T. Cumberbatch, J. Zuntz, H. K. K. Eriksen, and J. Silk, “Can the WMAP Haze really be a signature of annihilating neutralino dark matter?,” [arXiv:0902.0039](#) [[astro-ph.GA](#)].
- [45] N. Padmanabhan and D. P. Finkbeiner, “Detecting Dark Matter Annihilation with CMB Polarization : Signatures and Experimental Prospects,” *Phys. Rev.* **D72** (2005) 023508, [arXiv:astro-ph/0503486](#).
- [46] S. Galli, F. Iocco, G. Bertone, and A. Melchiorri, “CMB constraints on Dark Matter models with large annihilation cross-section,” [arXiv:0905.0003](#) [[astro-ph.CO](#)].
- [47] T. R. Slatyer, N. Padmanabhan, and D. P. Finkbeiner, “CMB Constraints on WIMP Annihilation: Energy Absorption During the Recombination Epoch,” [arXiv:0906.1197](#) [[astro-ph.CO](#)].
- [48] P. Grajek, G. Kane, D. Phalen, A. Pierce, and S. Watson, “Neutralino Dark Matter from Indirect Detection Revisited,” [arXiv:0807.1508](#) [[hep-ph](#)].
- [49] P. Grajek, G. Kane, D. Phalen, A. Pierce, and S. Watson, “Is the PAMELA Positron Excess Winos?,” [arXiv:0812.4555](#) [[hep-ph](#)].